Journal of Catalysis **184,** 298–302 (1999)
Article ID jcat.1999.2449, available online at http://www.idealibrary.com on IDEAL®

RESEARCH NOTE

High-Resolution Transmission Electron Microscopy Study of Carbon Deposited on the NiO/MgO Solid Solution Catalysts

Yun Hang Hu and Eli Ruckenstein[1]

Department of Chemical Engineering, State University of New York at Buffalo, Buffalo, New York 14260

Received October 8, 1998; revised February 8, 1999; accepted February 8, 1999

The carbon deposition due to the CH_4 decomposition at 790°C over NiO/MgO catalysts was investigated by high-resolution transmission electron microscopy. While no deposits could be detected over the catalysts with a NiO content smaller than 9.1 wt%, they were detected over the catalysts with NiO contents of 23 and 50 wt%. The carbon deposits are composed of platelets located at distances of about 0.34 nm, corresponding to the graphitic carbon. Various structures of the deposited carbon were observed: (a) carbon consisting of platelets parallel to the surface of the particle, which covers a catalyst particle, (b) nanotubes composed of platelets parallel to their axis, and (c) carbon vortexes consisting of platelets parallel to their axis.

Key Words: **NiO; MgO; solid solution; carbon deposition; HRTEM; lattice fringe.**

INTRODUCTION

During the past 20 years, CH_4 conversion to useful chemical compounds has become one of the most important topics of research in the catalytic area (1–10). Two main kinds of CH_4 conversions have been employed: direct and indirect conversion. The attempts for direct conversion of CH_4 have focused on the oxidative coupling to ethylene and ethane (6–8) and the oxygenation to methanol and formaldehyde (9, 10). Unfortunately, at the high temperatures (>700°C) necessary for high conversions, the formation of CO_2 is a highly favorable reaction ($\Delta G < -800$ kJ/mol). For this reason, in recent years there has been a renewed interest in the indirect conversion of CH_4 via the synthesis (CO/H_2) gas, which constitutes a feed stock for the methanol and Fischer–Tropsch syntheses (11, 12). Although the dominant commercial method employed to produce the synthesis gas is the steam reforming of methane ($CH_4 + H_2O \rightarrow CO + 3H_2$, $\Delta H = 225.4$ kJ/mol), this process provides either low conversion of CH_4 or low selectivity to CO and a too high H_2/CO product ratio for the methanol and the Fischer–Tropsch syntheses. Therefore, the research has centered on two other processes: the catalytic partial oxidation of methane ($CH_4 + 1/2O_2 \rightarrow CO + 2H_2$, $\Delta H = -38$ kJ/mol) and the CO_2 reforming of methane ($CH_4 + CO_2 \rightarrow 2CO + 2H_2$, $\Delta H = 247$ kJ/mol). Both reactions have high activity and selectivity, but the carbon deposition constitutes a serious problem in their industrial application. Although the carbon deposition has been widely investigated (13–16) as one of the mechanisms of catalyst deactivation, it is still difficult to inhibit the deposition without reducing the catalyst activity. Recently, we reported that the reduced NiO/MgO catalyst has high activity and selectivity at high space velocities, as well as excellent stability in the CO_2 reforming of methane (4b). In that reaction, the solid solution formed between support (MgO) and NiO could inhibit the carbon deposition. To better evaluate the ability of NiO/MgO solid solution catalysts to inhibit carbon deposition, the extreme case of deposition from a hydrocarbon (CH_4) free of any oxidant was investigated via high-resolution transmission electron microscopy (HRTEM).

EXPERIMENT

Catalyst

NiO/MgO catalysts were prepared by impregnating the support MgO (Aldrich) with an aqueous solution of nickel nitrate. The obtained paste was dried at room temperature in air, and then decomposed and calcined at 800°C in air for 1.5 h.

X-Ray Powder Diffraction

The solid solution of NiO/MgO was examined by X-ray powder diffraction (XRD) using a NICOLET X-ray diffraction instrument, equipped with a Cu$K\alpha$ source, at 40 kV and 20 mA.

CH_4 Decomposition

The CH_4 decomposition reaction was carried out for 3 h, at 790°C and atmospheric pressure, in a flow system at a

[1] To whom correspondence should be addressed.

0021-9517/99 $30.00

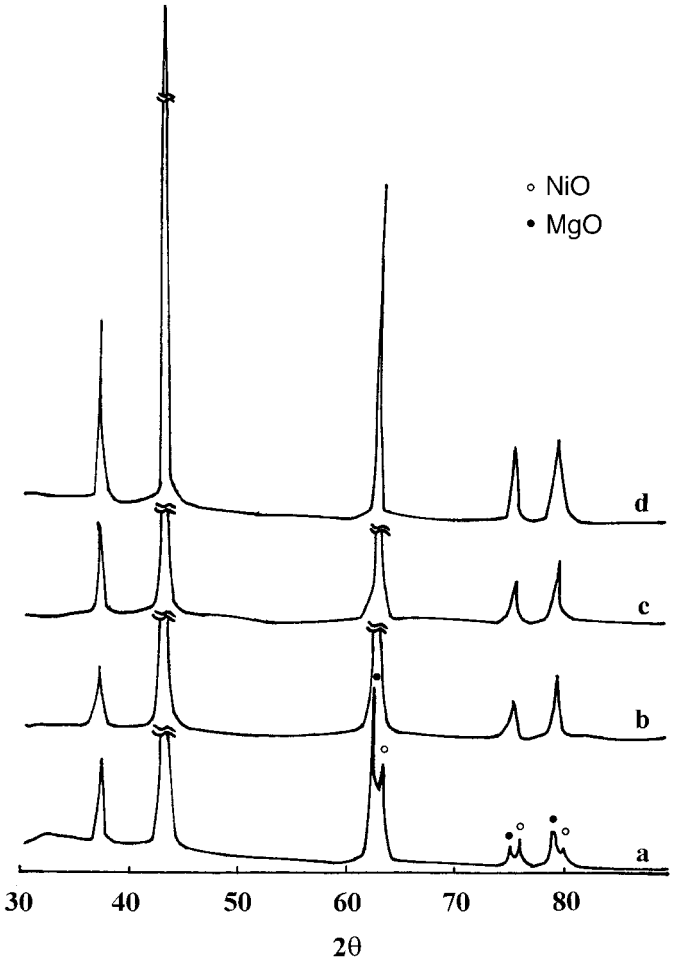

FIG. 1. XRD patterns of (a) mechanical mixture of NiO and MgO, (b) 9.1 wt% NiO/MgO catalyst, (c) 23 wt% NiO/MgO catalyst, and (d) 50 wt% NiO/MgO catalyst.

flow rate of 2 ml/min, using a vertical quartz tube (5 mm inside diameter) as reactor. The catalyst powder (weight: 0.5 g) was held on quartz wool.

High-Resolution Transmission Electron Microscope

The catalyst samples used for CH_4 decomposition were examined with a Jeol2010 transmission electron microscope operating at 200 kV, with a nominal point-to-point resolution of 1.9 Å. Suitable specimens were prepared by the ultrasonic dispersion of powder samples in acetone, followed by the location of drops of the resulting dispersions on copper grids covered with holey carbon support films.

RESULTS AND DISCUSSIONS

Phase Structure of NiO/MgO Catalyst and Carbon Deposition

The XRD patterns of MgO are similar to those of NiO. For MgO, $2\theta \approx 62.64$, 75.00, and 79.00 for the (220), (311), and (222) faces, respectively, while for NiO and the same faces they are by 0.6, 0.8, and 0.81°, respectively, greater. Therefore, the formation of a solid solution can be identified using the above three diffraction lines. Figure 1 compares a mechanical mixture of NiO and MgO with three NiO/MgO catalysts, and shows that the latter have three single peaks near the above 2θ values, while the former has three double peaks, one set for NiO and the other set, at lower 2θ values, for MgO. This indicates that a solid solution of NiO/MgO was indeed formed.

The carbon deposition on NiO/MgO catalysts due to the CH_4 decomposition was examined by HRTEM. For small amounts of NiO (<9.1 wt%), no carbon deposits could be detected (Fig. 2). In contrast, carbon deposition occurred (Figs. 3–6) over the 23 and 50 wt% NiO/MgO. This can be explained as follows: (i) NiO and MgO are face-centered cubic oxides with very close lattice parameters (4.1946 and 4.2112 Å for NiO and MgO, respectively). For this reason and as revealed by XRD (Fig. 1), MgO and NiO can form solid solutions. Because it is more difficult to reduce the NiO to Ni^0 in a solid solution (4a), only a small amount of Ni^0 is produced via NiO reduction by CH_4. The resulting Ni^0 atoms constitute the active sites. While we cannot bring direct evidence for the existence of Ni^0, indirect evidence was

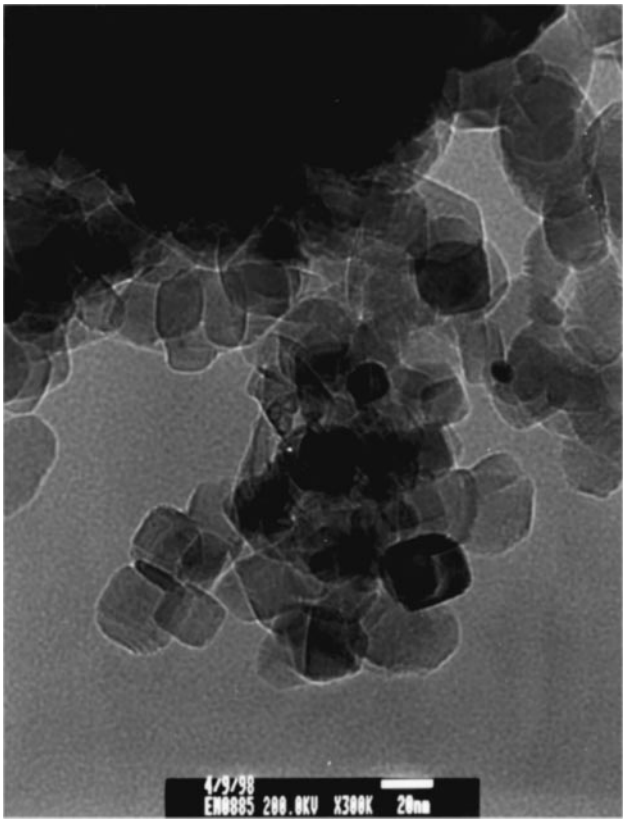

FIG. 2. TEM micrograph of the 9.1 wt% NiO/MgO catalyst used for CH_4 decomposition at 790°C.

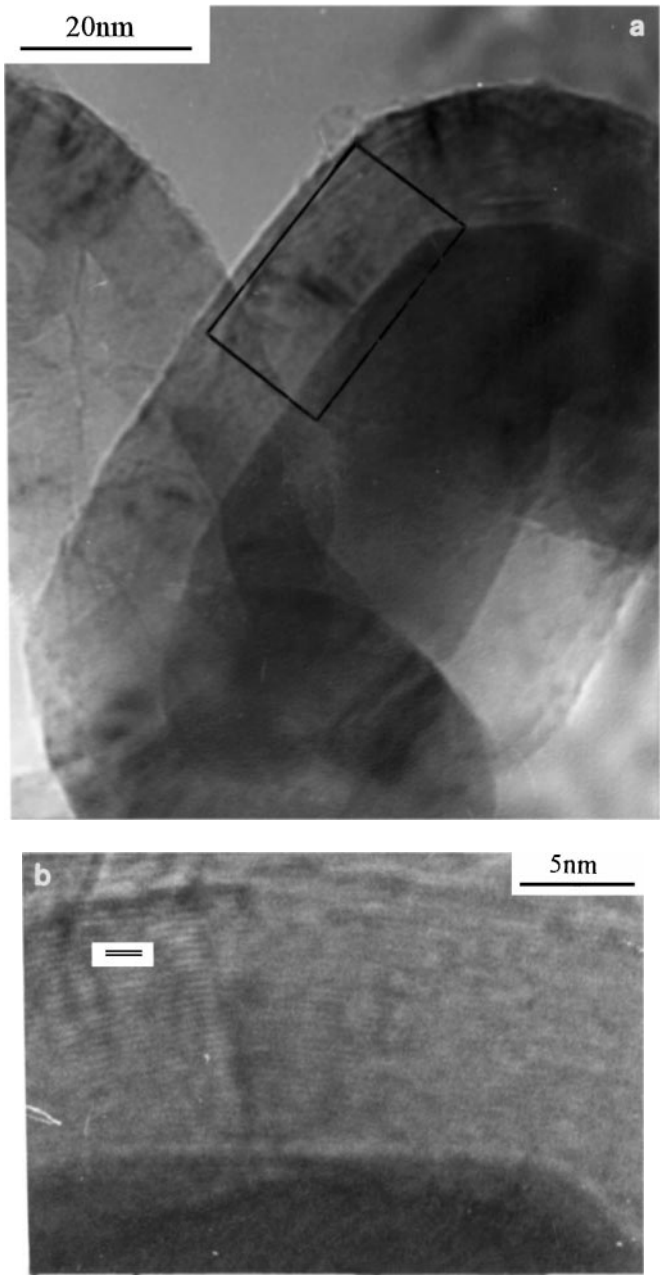

FIG. 3. (a) TEM micrograph which indicates the area displayed under (b); (b) high-resolution micrograph of the 23 wt% NiO/MgO catalyst used for CH_4 decomposition at 790°C. The carbon deposit is graphitic and consists of platelets oriented parallel to the catalyst particle surface.

provided by an isotopic study of the reaction of methane with the lattice oxygen of NiO/MgO (4c), which clearly demonstrated the reduction of NiO to Ni^0. The strong interactions between the highly dispersed Ni^0 and NiO/MgO inhibit the sintering of Ni. As a result, the solid solution catalyst has a high activity in the carbon dioxide reforming of methane (4). It has also high stability, because the clustering of Ni, which is necessary for coke formation, is prevented. However, as the content of Ni increases, the amount of NiO reduced increases, Ni clusters are generated, and coke can be formed. We showed in a previous paper that, for the CO_2 reforming of methane, the activity and stability of the NiO/MgO catalysts pass through maxima with increasing NiO content (4a).

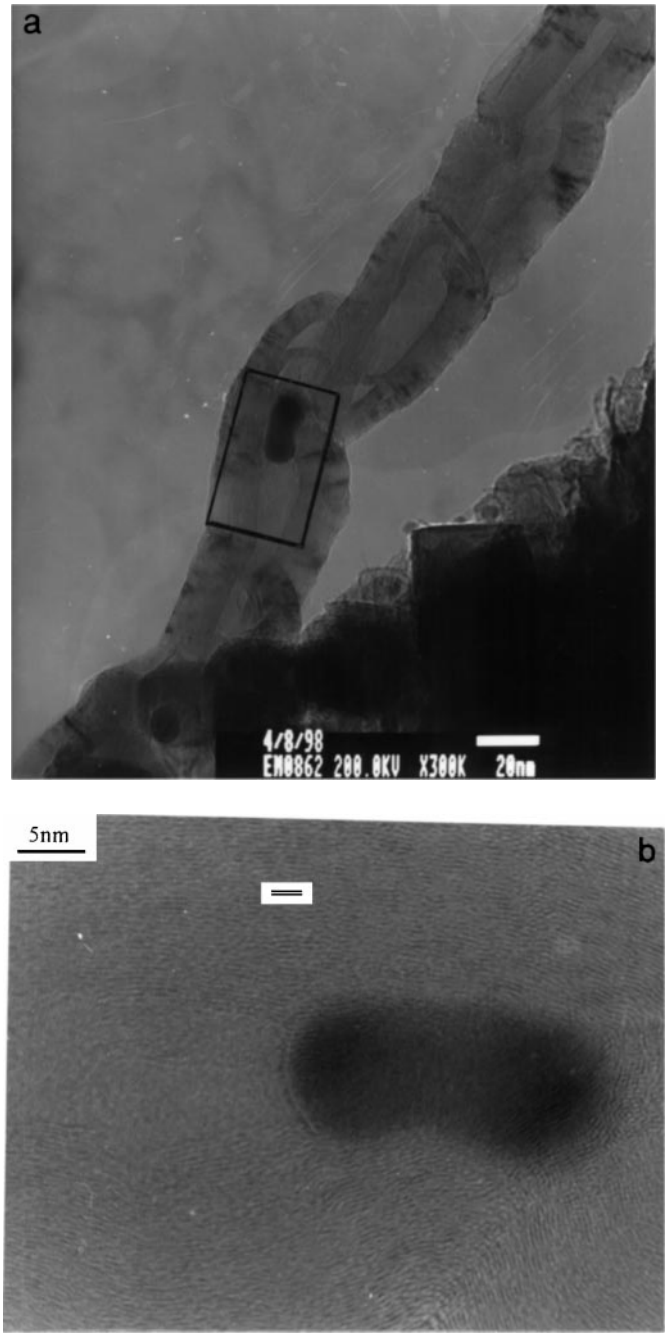

FIG. 4. (a) TEM micrograph; (b) high-resolution micrograph of the 23 wt% NiO/MgO catalyst used for CH_4 decomposition at 790°C. The carbon deposit is a graphitic nanotube consisting of platelets aligned parallel to the fiber axis.

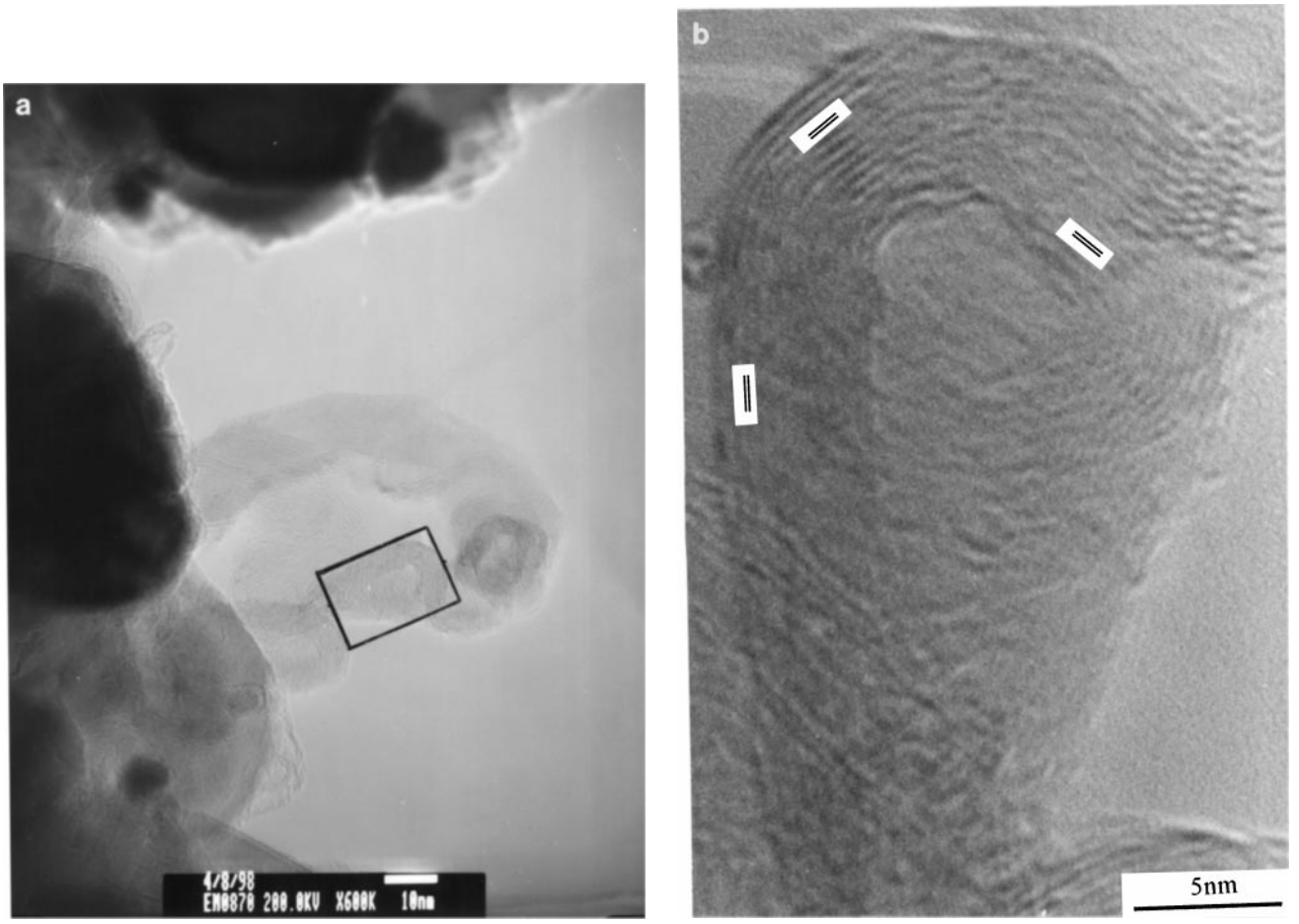

FIG. 5. (a) TEM micrograph; (b) high-resolution micrograph of the 23 wt% NiO/MgO catalyst used for CH_4 decomposition at 790°C. The carbon deposit is a graphitic vortex consisting of platelets parallel to its axis.

The Structure of Deposited Carbon

Various structures of the catalytically grown carbon were observed in the transmission electron micrographs (Figs. 3–6). Figures 3–5 represent micrographs of the 23 wt% NiO/MgO catalyst. They contain three kinds of carbon deposits. One kind of carbon, which covers the catalyst particle (Fig. 3a), is presented at a higher resolution in Fig. 3b. The lattice fringe image in the latter figure shows that the carbon deposit consists of platelets oriented parallel to the catalyst particle surface. The distance between the platelets, obtained from Fig. 3b, is about 0.34 nm, nearly the same as that of graphite (0.335 nm), indicating that this carbon is graphitic. The second kind of carbon is a hollow nanofiber (nanotube) (Fig. 4a), presented at a high resolution in Fig. 4b. It consists of carbon platelets aligned parallel to the fiber axis. The distance between the platelets is again about 0.34 nm, indicating that the hollow nanotube is also graphitic. It is worth noting that a catalyst particle is located in the hollow nanotube, with the same width as the hollow fiber, indicating that the inside diameter of the nanotube depends on the particle size of the catalyst. Obviously, the fiber was formed via a bi-directional precipitation of carbon on the opposite faces of the catalyst particle. The third kind of carbon, carbon vortexes (Fig. 5a), presented at a high resolution in Fig. 5b, consists of platelets parallel to the axis of the vortex, with a distance of about 0.34 nm between platelets, indicating again a graphitic structure.

The carbon growth over the catalyst particles depends on kinetic and thermodynamic factors. The kinetic factor is responsible for the various graphitic structures (17). However, the carbon growth is also affected by thermodynamic factors. The basal plan of graphite has a surface energy of $\sim$77 erg/cm^2 at 970°C, whereas a surface perpendicular to the former has a surface energy of over 4000 erg/cm^2 (16, 18). Therefore, the free energy of the system will be smaller when the graphite deposits consist of basal planes in contact with the particle and/or with the gas. This explains why the platelets of the nanotube are parallel to its axis. In addition, carbon deposits have been observed whose basal planes are predominantly parallel to the planes of the catalytic particle (Figs. 3a and 3b). This occurs because the interfacial free energies between the particle and the carbon deposit

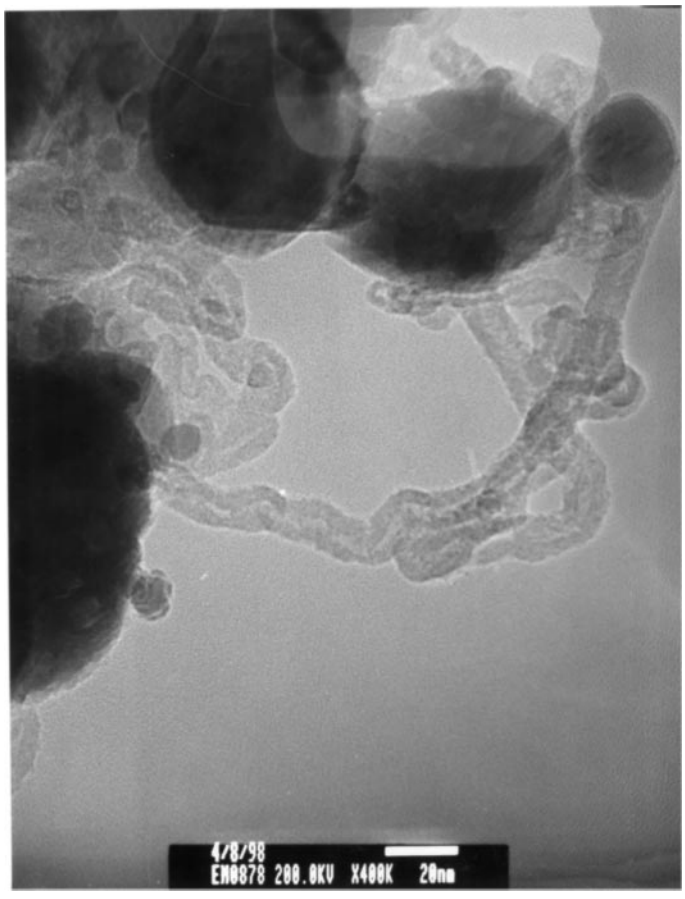

FIG. 6. TEM micrograph of the 50 wt% NiO/MgO catalyst used for CH_4 decomposition at 790°C. It contains a large amount of carbon.

and carbon deposit-gas are smaller for the basal plane of graphite than for any other plane (19, 20).

REFERENCES

1. Ashcroft, A. T., Cheetham, A. K., Foord, J. S., Green, M. L. H., Grey, C. P., Murrell, A. J., and Vernon, P. D. F., *Nature* **344**, 319 (1990).
2. Dissanayake, D., Rosynek, M. P., and Lunsford, J. H., *J. Catal.* **132**, 117 (1991).
3. Hickman, D. A., and Schmidt, L. D., *J. Catal.* **138**, 267 (1992).
4. (a) Hu, Y. H., and Ruckenstein, E., *Catal. Lett.* **36**, 145 (1996); *J. Catal.* **158**, 260 (1996); (b) Ruckenstein, E., and Hu, Y. H., *Appl. Catal. A* **133**, 149 (1995); *Appl. Catal. A* **154**, 185 (1997); (c) Hu, Y. H., and Ruckenstein, E., *Catal. Lett.*, 1999 (in press).
5. Rostrup-Nielsen, J. R., and Hansen, J.-H. B., *J. Catal.* **144**, 38 (1993).
6. Keller, G. E., and Bhasin, M. M., *J. Catal.* **73**, 9 (1982).
7. Lunsford, J. H., *Stud. Surf. Sci. Catal.* **81**, 1 (1994).
8. Ruckenstein, E., and Khan, A. Z., *J. Catal.* **141**, 628 (1993).
9. Hall, T. J., Hargreaves, J. S. J., Hutchings, G. J., Joyner, R. W., and Taylor, S. H., *Fuel Processing Technol.* **42**, 151 (1995).
10. Pitchai, R., and Klier, K., *Catal. Rev. Sci. Eng.* **28**, 13 (1986).
11. Bart, J. C. J., and Sneeden, R. P. A., *Catal. Today* **2**, 1 (1987).
12. Vannice, M. A., *Catal. Rev. Sci. Eng.* **14**, 153 (1976).
13. Baker, R. T. K., Barber, M. A., Harris, P. S., Feates, F. S., and Waite, R. J., *J. Catal.* **26**, 51 (1972).
14. Rostrup-Nielsen, J. R., *J. Catal.* **33**, 184 (1974).
15. Baker, R. T. K., Gadsby, G. R., and Terry, S., *Carbon* **13**, 245 (1975).
16. Tibbets, G. G., *J. Crystal Growth* **66**, 632 (1984).
17. Rodriguez, Nelly M., Chambers, A., and Baker, R. T. K., *Langmuir* **11**, 3862 (1995).
18. Abrahamson, J., *Carbon* **11**, 337 (1973).
19. Lee, S. H., and Ruckenstein, E., *J. Catal.* **107**, 23 (1987).
20. Ruckenstein, E., "Metal-Support Interactions in Catalysis, Sintering, and Redispersion" (S. A. Stevenson, J. A. Dumesic, R. T. K. Baker, and E. Ruckenstein, Eds.), p. 141, Van Nostrand–Reinhold, New York, 1987.